

Dynamic freezing of strongly correlated ultracold bosons

S. Mondal⁽¹⁾, D. Pekker⁽²⁾, and K. Sengupta⁽¹⁾

⁽¹⁾ *Theoretical Physics Department, Indian Association for the Cultivation of Science, Jadavpur, Kolkata-700032, India.*

⁽²⁾ *Department of Physics, California Institute of Technology, Pasadena, California-91125, USA.*

(Dated: March 13, 2021)

We study the non-equilibrium dynamics of ultracold bosons in an optical lattice with a time dependent hopping amplitude $J(t) = J_0 + \delta J \cos(\omega t)$ which takes the system from a superfluid phase near the Mott-superfluid transition ($J = J_0 + \delta J$) to a Mott phase ($J = J_0 - \delta J$) and back through a quantum critical point ($J = J_c$) and demonstrate dynamic freezing of the boson wavefunction at specific values of ω . At these values, the wavefunction overlap F (defect density $P = 1 - F$) approaches unity (zero). We provide a qualitative explanation of the freezing phenomenon, show it's robustness against quantum fluctuations and the presence of a trap, compute residual energy and superfluid order parameter for such dynamics, and suggest experiments to test our theory.

PACS numbers: 64.60.Ht, 05.30.Jp, 05.30.Rt

Theoretical study of non-equilibrium dynamics in closed quantum systems has seen great progress in recent years [1] mainly due to the possibility of realization of such dynamics using ultracold atom in optical lattices [2, 3]. For bosonic atoms, such systems are well described by the Bose-Hubbard model with on-site interaction strength U and nearest neighbor hopping amplitude J [4, 5]. Several theoretical studies have been carried out on the quench and ramp dynamics of this model [6–11]; some of them have also received support from recent experiments [3]. In contrast, studies on periodically driven closed quantum systems have been undertaken in the past mainly on driven two-level systems [12, 13] or on weakly interacting or integrable many-body systems which can be modeled by them [14, 15]. Among these, Ref. [15] has predicted freezing of the time-averaged value of the order parameter (magnetization) of an periodically driven one-dimensional (1D) Ising or XY model, when the temporal average is performed over several drive cycles, at specific drive frequencies. Such a freezing occurs in the high frequency regime and exhibits non-monotonic dependence on the drive frequency. However, to the best of our knowledge, the phenomenon of dynamic freezing has never been demonstrated for dynamics involving a single drive cycle and/or for non-integrable quantum systems. Recent studies of periodic dynamics of the Bose-Hubbard model have not addressed this issue [16, 17].

In this work, we demonstrate, via designing a periodic driving protocol, that the periodically driven Bose-Hubbard model may exhibit dynamic freezing of the boson wavefunction $|\psi(t=0)\rangle = |\psi(t=T)\rangle$ for specific values of the drive frequencies $\omega = 2\pi/T$. Our driving protocol constitutes a time-dependent hopping amplitude of the bosons $J(t) = J_0 + \delta J \cos(\omega t)$ with J_0 and δJ chosen such that the drive takes the system from a superfluid (SF) ($J = J_0 + \delta J$) to the Mott insulator (MI) state ($J = J_0 - \delta J$) and back through the tip of the Mott lobe where $\mu = \mu_{\text{tip}}$. We demonstrate, using mean-field theory, that such a freezing phenomenon de-

rives from quantum interference of the dynamic phases acquired by the bosons and compute the defect formation probability $P = 1 - F$ (where $F = |\langle\psi(t=0)|\psi(t=T)\rangle|^2$ is the wavefunction overlap), the superfluid order parameter $\Delta(T) = \langle\psi(T)|b|\psi(T)\rangle$ (where b denotes the boson annihilation operator), and the residual energy $Q = E(t=T) - E_G$ (where $E(t=T)$ is the energy of the system at the end of the drive cycle and E_G is the initial ground state energy) as a function of ω . We also show, via inclusion of quantum fluctuation by a projection operator approach [11] and numerical mean-field study of a trapped boson system that the freezing phenomenon is qualitatively robust against quantum fluctuations and the presence of a trap. We note that such a freezing behavior has two novel characteristics which distinguishes it from its counterpart in Ref. [15]. First it does not need high frequencies as $\hbar\omega/U \ll 1$ throughout the range of ω where the freezing occurs. Second, it occurs for a single cycle of the drive and does not need averaging over several cycles. Such a dynamic freezing phenomenon has not been studied in the context of closed quantum systems; our work therefore constitutes a significant advance in our understanding of periodic dynamics of closed non-integrable quantum systems.

The Hamiltonian describing a system of ultracold bosonic atoms confined by a trap and in an optical lattice is given by

$$\mathcal{H} = \sum_{\langle \mathbf{r}, \mathbf{r}' \rangle} -J b_{\mathbf{r}}^\dagger b_{\mathbf{r}'} + \sum_{\mathbf{r}} [-\mu_{\mathbf{r}} \hat{n}_{\mathbf{r}} + \frac{U}{2} \hat{n}_{\mathbf{r}} (\hat{n}_{\mathbf{r}} - 1)] \quad (1)$$

where $\mu_{\mathbf{r}}$ denotes the chemical potential at site \mathbf{r} , \mathbf{r}' denotes one of the z nearest neighboring sites of \mathbf{r} , and $\hat{n}_{\mathbf{r}} = b_{\mathbf{r}}^\dagger b_{\mathbf{r}}$. In the absence of a trap, $\mu_{\mathbf{r}} = \mu$ for all sites and for $zJ \ll U$, the ground state of the model is a MI state with \bar{n} bosons per site with $\bar{n} = 1$ for $0 \leq \mu/U \leq 1$. For $zJ \gg U$, the bosons are delocalized and the system, for $d \geq 2$, is in a SF state. In between, at $J = J_c$, the system undergoes a SF-MI transition. The equilibrium phase diagram of the model constitutes the well-known

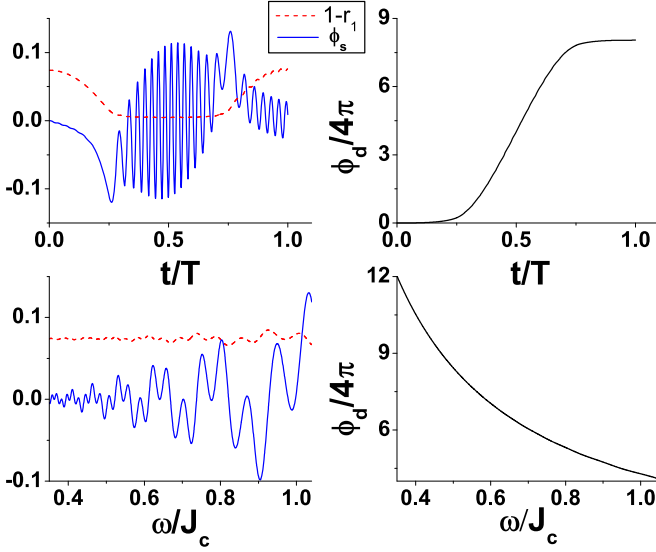


FIG. 1: (Color online) Top left panel: Plot of $1 - r_1(t)$ (red dashed line) and $\phi_s(t)$ (blue solid line) as a function of t . Bottom left panel: Variation of $1 - r_1(T)$ (red dashed line) and $\phi_s(T)$ (blue solid line) with ω . Top (Bottom) right panel: Plot $\phi_d(t)$ ($\phi_d(T)$) as a function of t (ω). For all plots $J_0 = 1.05J_c$, $\delta J = 0.35J_c$, and $\mu = 0.414U$.

Mott lobe structure [4, 5].

To obtain an semi-analytic insight to the freezing phenomenon, we first analyze the periodically driven Bose-Hubbard model in the absence of a trap and within mean-field approximation. The time-dependent mean-field Hamiltonian is given by

$$\mathcal{H}_{\text{mf}} = \sum_{\mathbf{r}} [-\mu \hat{n}_{\mathbf{r}} + \frac{U}{2} \hat{n}_{\mathbf{r}}(\hat{n}_{\mathbf{r}} - 1)] + (\Delta'_r(t) b_r^\dagger + \text{h.c.}) \quad (2)$$

where $\Delta'_r(t) = -J(t) \sum_{\langle r, r' \rangle} \langle b_{r'} \rangle$ and $\Delta'_0 = \Delta'(t=0)$. Within homogeneous mean-field theory, the Gutzwiller wavefunction for the bosons reads $|\psi(\mathbf{r}, t)\rangle_{\text{mf}} = \prod_{\mathbf{r}} \sum_n f_n(t) |n\rangle$ [18]. The Schrodinger equation $i\partial_t |\psi(\mathbf{r}, t)\rangle_{\text{mf}} = \mathcal{H}_{\text{mf}}(t) |\psi(\mathbf{r}, t)\rangle_{\text{mf}}$ yields the time-dependent mean-field equations for $f_n(t) \equiv f_n$:

$$(i\partial_t - E_n) f_n = \tilde{\Delta}(t) \sqrt{n} f_{n-1} + \tilde{\Delta}^*(t) \sqrt{n+1} f_{n+1}, \quad (3)$$

where $\tilde{\Delta}(t) = -zJ(t) \sum_n \sqrt{n} f_{n-1}^* f_n$, and $E_n = -\mu n + U(n-1)n/2$. In what follows, we shall choose J_0 and δJ such that the ground state of H_{mf} with $J = J_0 + \delta J$ is a SF state close to the QCP so that $f_n(t=0) \simeq 0$ for $n \geq 3$ and $f_1(t=0) \gg f_0(t=0), f_2(t=0)$. As can be verified by explicit numerics, in this regime $f_n(t)$ for $n \geq 3$ remains small for all t during the dynamics and can thus be neglected. The equations for f_0, f_1 and f_2 then reads (suppressing time dependence of $f_n(t)$ for clarity)

$$\begin{aligned} i\partial_t f_0 &= -zJ(t) [|f_1|^2 f_0 + \sqrt{2} f_2^* f_1^2] \\ i\partial_t f_2 &= E_2 f_2 - zJ(t) [2|f_1|^2 f_2 + \sqrt{2} f_0^* f_1^2] \\ i\partial_t f_1 &= E_1 f_1 - zJ(t) [(2|f_2|^2 + |f_0|^2) f_1 + 2\sqrt{2} f_1^* f_2 f_0]. \end{aligned} \quad (4)$$

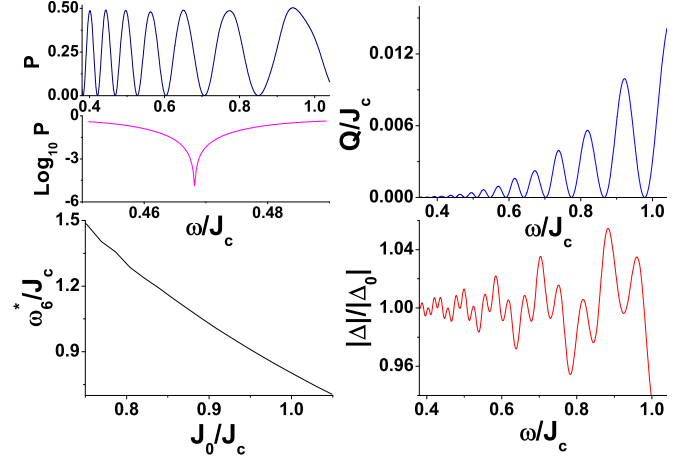


FIG. 2: (Color online) Top left panel: Plot of the defect density P as a function of ω/J_c displaying freezing at $\omega = \omega_m^*$. Inset shows $\text{Log}_{10} P$ near $\omega_m^* \simeq 0.47J_c$. Bottom left panel: Variation of ω_m/J_c as a function of J_0/J_c for $m = 6$. Right panels: Plot of Q and $|\Delta(T)|$ as a function of ω/J_c . All parameters are same as Fig. 1.

From Eqs. 4, it is easy to see that $|f_n|$, for $n \leq 2$, obeys the relation $\partial_t |f_0|^2 = \partial_t |f_2|^2 = -\partial_t |f_1|^2/2$. Parameterizing $f_n = r_n(t) \exp[i\phi_n(t)]$, with the choice that $\phi_n(0) = 0$ and $r_n(0) = f_n(0)$, one can write

$$r_{2[0]}^2(t) = -(r_1^2(t) - 1)/2 + [-]\eta, \quad (5)$$

where η is a time independent parameter whose value is fixed by the initial values r_n [19]. Note that η represents the magnitude of the particle-hole asymmetry since $r_0 = r_2$ for $\eta = 0$. Substituting Eq. 5 in Eq. 4, we get

$$\begin{aligned} \partial_t r_1 &= -\sqrt{2} z J(t) \sin(\phi_s) r_1 g_0(r_1), \\ \partial_t \phi_s &= -U + z J(t) [g_1(r_1) - g_2(r_1) \cos(\phi_s)], \\ \partial_t \phi_d &= -U + 2\mu + z J(t) r_1^2 \left[1 - 4\sqrt{2} \eta \cos(\phi_s) / g_0(r_1) \right], \end{aligned} \quad (6)$$

where we have suppressed the time dependence of r_1 and $\phi_{s(d)}$ for clarity, $\phi_s = \phi_0 + \phi_2 - 2\phi_1$ and $\phi_d = \phi_2 - \phi_0$ are the sum and differences of the relative phases of the Gutzwiller wavefunction, and the functions $g_i(r_1)$ are given by

$$\begin{aligned} g_0(r_1) &= \sqrt{(1 - r_1^2)^2 - 4\eta^2}, \quad g_1(r_1) = 6r_1^2 - 3 - 2\eta, \\ g_2(r_1) &= 2\sqrt{2} [r_1^2(r_1^2 - 1)/g_0(r_1) + g_0(r_1)]. \end{aligned} \quad (7)$$

We note that the first two of the equations in Eq. 6 are coupled equations describing the evolution of r_1 and ϕ_s , while the third describes the evolution of ϕ_d in terms of r_1 and ϕ_s . Furthermore, using a scaled variable $t' = \omega t / (2\pi)$, we find that the relation between r_1 and ϕ_s can be written as

$$dr_1/d\phi_s = \frac{-\sqrt{2} \sin(\phi_s) r_1 g_0(r_1)}{[g_1(r_1) - g_2(r_1) \cos(\phi_s)] - U/zJ(t')}. \quad (8)$$

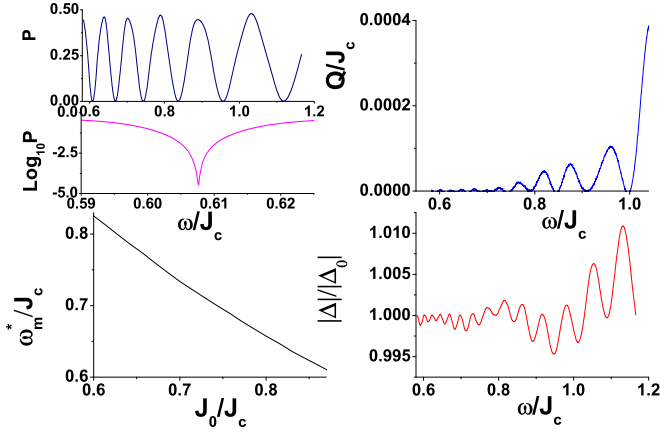


FIG. 3: (Color online) Similar plots as in Fig. 2 but with $J_0[\delta J] = 0.87[0.58]J_c$ and computed using the projection operator approach displaying robustness of the freezing phenomenon against quantum fluctuations. See text for details.

This allows us to symbolically write $\phi_s = \xi(r_1, t')$, where ξ is an unknown function, and thus establish an ω independent relation between r and ϕ_s for any fixed t' .

Eqs. 5, 6 and 7 constitute the central result of this work. They constitute a complete description of the evolution of f_0 , f_1 , and f_2 in the presence of the periodic drive and provide an understanding of the freezing phenomenon as follows. First, we find that a numerical solution of Eq. 6, together with Eq. 5, allows us to obtain r_n , ϕ_s and ϕ_d as a function of time. A plot of $1 - r_1(t)$ and $\phi_s(t)$ as a function of t for $\omega/J_c = 0.52$ is shown in the left panel of Fig. 1. We find that r_1 changes appreciably when $J(t)$ is close to J_c ; however, $r_1(T) \simeq r_1(0)$ at the end of the evolution. Note that this also implies, via Eq. 5, that $r_{2(0)}(0) \simeq r_{2(0)}(T)$. The bottom left panel of Fig. 1 shows that the relation $r_1(T) \simeq r_1(0)$ holds for a significant range $\omega/J_c \leq 0.8$. Second, we note that, $\phi_s(t)$ undergoes rapid oscillation when $J(t) \leq J_c$; however, it also comes back close to its initial value at the end of the drive: $\phi_s(T) \simeq \phi_s(0)$. Since ϕ_s and r_1 satisfies a ω independent relation, $\phi_s = \xi(r_1, t')$, we infer that ϕ_s must remain close to its initial value for the same range of ω for which $r_1(T) \simeq r_1(0)$; this is verified numerically in the bottom left panel of Fig. 1. Finally, we note, from the right panels of Fig. 1, that $\phi_d(T)$ is a monotonic function of ω . Thus we may define $\omega = \omega_m^*$ for which $\phi_d(T) \simeq 4\pi m$ (m being an integer). Together with the fact that $r_1(T) \simeq r_1(0)$ and $\phi_s(T) \simeq \phi_s(0) = 0$, we find that at $\omega = \omega_m^*$, both the relative phases satisfy $\phi_2 - \phi_1 = -(\phi_0 - \phi_1) \simeq 2\pi m$ leading to $|\psi_{mf}(T)\rangle \simeq |\psi_{mf}(0)\rangle$ up to a global phase. This constitutes the dynamics freezing of $|\psi\rangle_{mf}$.

To obtain an accurate estimate of the degree of freezing, we compute the defect density $P = 1 - F = 1 - |\langle \psi_{mf}(T) | \psi_{mf}(0) \rangle|^2$. The plot of P as a function of ω clearly shows that $P \rightarrow 0$ at $\omega = \omega_m^*$. A plot of $\text{Log}_{10} P$ vs ω near $\omega_m^*/J_c \simeq 0.47$, shown in the top left panel of

Fig. 2 reveals that $P \sim 10^{-6}$ indicating that the overlap, up to a global phase, is exact within our numerical accuracy. We have checked for all $\omega_m^* \leq 0.8J_c$, $P < 10^{-4}$ which indicates a near perfect freezing. We also compute the residual energy $Q(T)$ and the SF order parameter

$$\Delta = r_1 e^{i\phi_d/2} \left(r_0 e^{-i\phi_s/2} + \sqrt{2} r_2 e^{i\phi_s/2} \right), \quad (9)$$

at $t = T$ as a function of ω . We find from Eq. 9 that $|\Delta|$ is independent of ϕ_d . Thus $|\Delta(T)|/|\Delta_0|$ and Q/U (which can also be shown to be independent of ϕ_d) remain close to unity and zero respectively over the entire range of ω/J for which r_1 and ϕ_s remain close to their initial values as shown in right panels of Fig. 2. Such a behavior distinguishes these quantities from P which depends on ϕ_d and hence vanishes at discrete ω_m . Finally, we find that for all values of J_0 shown in bottom left panel of Fig. 2, there is an appreciable range of ω/J_c within which the freezing phenomenon occurs and that ω_m^* decreases monotonically as a function of J_0 over this range.

Next, we study the effect of quantum fluctuations on the freezing phenomenon. We incorporate such fluctuations by using a projection operator method developed in Ref. 11 which provides an accurate treatment of dynamics with fluctuations for $zJ(t)/U \ll 1$. The idea behind this approach, as detailed in Ref. 11, is to introduce a projection operator $P_\ell = |n_0\rangle\langle n_0|_{\mathbf{r}} \times |n_0\rangle\langle n_0|_{\mathbf{r}'}$ which lives on the link ℓ between the neighboring sites \mathbf{r} and \mathbf{r}' of the lattice. Using P_ℓ , one can write the boson hopping term as $T' = \sum_{\langle \mathbf{r}\mathbf{r}' \rangle} -J(t)b_{\mathbf{r}}^\dagger b_{\mathbf{r}'} = \sum_\ell T'_\ell = \sum_\ell [(P_\ell T'_\ell + T'_\ell P_\ell) + P_\ell^\perp T'_\ell P_\ell^\perp]$ where $P_\ell^\perp = (1 - P_\ell)$. In the strong-coupling regime where $zJ(t)/U \ll 1$, the term $T'_\ell{}^0[J] = (P_\ell T'_\ell + T'_\ell P_\ell)$, at any instant, represents hopping processes which takes the system out of the instantaneous low-energy manifold. Thus one can devise a time-dependent canonical transformation via an operator $S \equiv S[J(t)] = \sum_\ell -i[P_\ell, T'_\ell]/U$ which eliminates $T'_\ell{}^0[J(t)]$ up to first order in $J(t)/U$ and leads to the effective instantaneous time-dependent Hamiltonian $H^* = \exp(-iS[J(t)])\mathcal{H}\exp(iS[J(t)])$. Such a canonical transformation is equivalent to a transformation on the system wavefunction $|\psi\rangle$: $|\psi'\rangle = \exp(-iS[J(t)])|\psi\rangle$. We note that $|\psi\rangle$ and $|\psi'\rangle$ coincides for $J = 0$ which leads us to the natural choice $|\psi'\rangle = \prod_{\mathbf{r}} \sum_n f_{\mathbf{r}}^n(t)|n_{\mathbf{r}}\rangle$. Note that $|\psi\rangle$ is not of Gutzwiller form; it involves spatial correlation due to $\exp(iS[J(t)])$ factor. The instantaneous energy of the system is given by $E[\{f_{\mathbf{r}}^n(t)\}] = \langle \psi | \mathcal{H} | \psi \rangle = \langle \psi' | H^* | \psi' \rangle + O(J(t)^3/U^3)$ and includes $O(J^2/U^2)$ quantum fluctuation corrections. As shown in Ref. [11], this formalism allows one to describe the dynamics of the bosons by solving for the Schrodinger equation for $|\psi'\rangle$:

$$(i\hbar\partial_t + \partial S[J(t)]/\partial t)|\psi'\rangle = H^*[J(t)]|\psi'\rangle. \quad (10)$$

Using the expression of $|\psi'\rangle$ and $E[\{f_{\mathbf{r}}^n\}]$, one can convert Eq. 10 to a set of equations for $\{f_{\mathbf{r}}^n(t)\}$ [11]. Defining

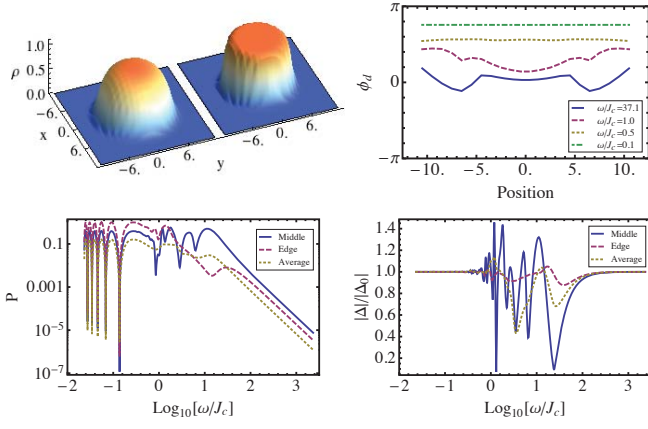


FIG. 4: (Color online) Top left panel: Plot of the boson density profile in the trap at $t = 0$ (left) and $t = T$ (right). Top right panel: Variation of relative phase $\phi_d(T)$ as a function of the position (along $y = 0$) in the trap displaying coherent evolution of the bosons. Bottom panels: Plot P and $|\Delta(T)|/|\Delta_0|$ as a function ω displaying freezing phenomenon at ω_m^* . For all plots $J_0 = 0.04U$, $\delta J = 0.015U$, $J_c = 0.041U$, and $\mu_0 = 0.415U$.

$\varphi_n = \sqrt{n+1}f_n^*f_{n+1}$, one gets

$$\begin{aligned} i\hbar\partial_t f_n &= \delta E[\{f_n(t)\}; J(t)]/\delta f_n^* + \frac{iz\hbar}{U} \frac{\partial J(t)}{\partial t} \\ &\times \left(\sqrt{n}f_{n-1} \left[\delta_{n\bar{n}}\varphi_{\bar{n}} - \delta_{n,\bar{n}+1}\varphi_{\bar{n}-1} \right] \right. \\ &\left. + \sqrt{n+1}f_{n+1} \left[\delta_{n\bar{n}}\varphi_{\bar{n}-1}^* - \delta_{n,\bar{n}-1}\varphi_{\bar{n}}^* \right] \right) \end{aligned} \quad (11)$$

A numerical solution of Eq. 11 yields $f_n(t)$ and hence $|\psi'\rangle$ using which one can compute $|\psi(t)\rangle = \exp[iS]|\psi'(t)\rangle$ perturbatively to $O[J(t)^2/U^2]$. Similarly, expectation value of any operator O at any instant t can be calculated in terms of $|\psi'(t)\rangle$: $\langle O \rangle = \langle \psi'(t) | e^{-iS} O e^{iS} | \psi'(t) \rangle = \langle \psi'(t) | O | \psi'(t) \rangle - \langle \psi'(t) | [iS, O] | \psi'(t) \rangle + \dots$, where the ellipsis indicate higher order terms in $J(t)/U$. Note that the second term in the expression originates from quantum fluctuation and modifies mean-field result (first term). Using the above-mentioned procedure detailed in Ref. [11], we compute $P(T)$, $Q(T)$ and $|\Delta(T)|$ as shown in Fig. 3. We find that key effects of the quantum fluctuations is to change numerical values of ω_m^* and the precise range of ω over which freezing occurs; however the mean-field results hold qualitatively in the sense that $P \rightarrow 0$ for several ω_m^* with $\text{Log}_{10}P \leq -4$ for all ω_m^* . Further ω_m^* also decreases monotonically with J_0 as shown in left bottom panel of Fig. 3 for $\omega^* \simeq 0.6J_c$.

Finally, we consider the effect of a harmonic trap on the freezing phenomenon. For this part, we numerically solve Eq. 3 for $d = 2$ with $\mu_{\mathbf{r}} = \mu_0 + 0.01U[(\mathbf{r}_x - 1/2)^2 + (\mathbf{r}_y - 1/2)^2]$, for $N_0 = 576$ sites (linear dimension 24) and with fixed total particle number N_0 . We choose the trap parameters so that the ground state of the bosons in center of the trap at $t = T/2$ is MI phase with $\bar{n} = 1$. The evolution of the density profile of the bosons is shown in

the top left panel of Fig. 4 for $t = 0$ (left) and $t = T/2$ (right). The top right panel indicates evolution of ϕ_d as a function of the position of the bosons in the trap along the line $y = 0$. The plot indicates that for all $\omega \leq J_c$, ϕ_d evolves coherently with negligible spatial variation. The plots for ϕ_s and r_1 are similar in nature; thus, we expect the boson evolution to have the same qualitative properties as that found within a homogeneous mean-field approach. A plot of P ($|\Delta(T)|/|\Delta_0|$) as a function of $\text{Log}_{10}(\omega/J_c)$ in the lower left (right) panels of Fig. 4 confirms this expectation. We find that the main effect of the trap is to push the freezing phenomenon to lower frequencies leaving its qualitative nature unchanged. The largest freezing frequency occurs at $\simeq 0.2J_c$ which is large compared to frequencies $\simeq 0.05J_c$ where momentum conserving boson pair production at finite momenta, which is not captured within mean-field theory, is expected to become significant [20]. Fig. 4 also demonstrates that the freezing phenomenon disappears at higher drive frequencies where the trapped bosons do not evolve coherently leading to spatial variation of ϕ_d .

For experimental verifications of our work, we suggest interference of two bosonic condensates in the presence of an optical lattice, near the QCP which are separated after creation by a double-well potential and allowed to evolve separately for a fixed holdout time. It is well known that recombination of such separated condensates can act as a readout scheme for their relative phases [21]. We propose such a readout when one of the condensates is driven periodically with a frequency ω during the holdout for a single period $T = 2\pi/\omega$. Our specific prediction is that the relative phase measured for such a drive with $\omega = \omega_m^*$ is going to match the phase without any drive indicating dynamic freezing. For all such experiments one needs to estimate an optimal temperature T_0 at which they can be carried out. The typical value of U deep inside the Mott phase is $\simeq 2\text{KHz} = 200\text{nK}$ leading to a melting temperature of $T_m \simeq 0.2U = 40\text{nK}$ for $d = 3$. The SF phase near the Mott tip has a coherence temperature of $T_c \simeq zJ_c \simeq 35\text{nK}$ [22]. Thus a temperature of a few nano-Kelvins ($T_0 \ll T_m, T_c$), which is currently within the experimental reach, would be ideal for testing our prediction.

In conclusion, we have demonstrated that periodic dynamics of the ultracold bosons described by the Bose-Hubbard model leads to dynamic freezing of the Boson wavefunction at specific drive frequencies which are determined by the condition $\phi_d(T) = 4\pi m$. The freezing phenomenon is qualitatively robust against the presence of the trap and quantum fluctuations; it manifests itself at discrete drive frequencies $\omega_m^* \leq J_c$ via presence of dips in the defect density and can be detected by suitable interference experiments.

SM and KS thanks K. Ray for several stimulating discussions. KS thanks DST for support through grant SR/S2/CMP-001/2009. DP acknowledges support from

the Lee A. DuBridge fellowship.

-
- [1] A. Polkovnikov *et al.*, Rev. Mod. Phys. **83**, 863 (2011); J. Dziarmaga, Adv. Phys. **59**, 1063 (2010).
 - [2] M. Greiner, *et al.*, Nature **415**, 39 (2002); C. Orzel *et al.*, Science **291**, 2386 (2001); Kinoshita, T., T. Wenger, and D. S. Weiss, Nature **440**, 900 (2006); L. E. Sadler *et al.*, Nature **443**, 312 (2006).
 - [3] W.S. Bakr *et al.*, Science **329**, 547 (2010).
 - [4] D. Jaksch *et al.*, Phys. Rev. Lett. **81**, 3108 (1998); K. Sengupta and N. Dupuis, Phys. Rev. A **71**, 033629 (2005); J. Freericks *et al.*, Phys. Rev. A **79**, 053631 (2009).
 - [5] W. Krauth and N. Trivedi, Europhys. Lett. **14**, 627 (1991); B. Caprogrosso-Sansone, N. Prokofiev, and B. V. Svistunov, Phys. Rev. B **75**, 134302 (2007).
 - [6] C. Kollath, A. Lauchli, and E. Altman, Phys. Rev. Lett. **98**, 180601 (2007).
 - [7] C. De Grandi, V. Gritsev, A. Polkovnikov, Phys. Rev. B **81**, 224301 (2010); C. De Grandi, R. A. Barankov, and A. Polkovnikov, Phys. Rev. Lett. **101**, 230402 (2008); C. De Grandi, V. Gritsev, and A. Polkovnikov, Phys. Rev. B **81**, 012303 (2010); C. de Grandi and A. Polkovnikov, *Quantum Quenching, Annealing and Computation*, Eds. A. Das, A. Chandra and B. K. Chakrabarti, Lect. Notes in Phys., **802** (Springer, Heidelberg 2010).
 - [8] A. Polkovnikov, Phys. Rev. A **66**, 053607 (2002); A. Polkovnikov and V. Gritsev, Nat. Phys. **4**, 477 (2006).
 - [9] E. Altman and A. Auerbach, Phys. Rev. Lett. **89**, 250404 (2002).
 - [10] R. Schutzhold *et al.*, Phys. Rev. Lett. **97**, 200601 (2006); J. Wernsdorfer *et al.* Phys. Rev. A **81**, 043620 (2010).
 - [11] C. Trefzger and K. Sengupta, Phys. Rev. Lett. **106** 095706 (2011); A. Dutta, C. Trefzger, and K. Sengupta, arXiv:1111.5085 (unpublished).
 - [12] S.N. Shevchenko, S. Ashhab, and F. Nori, Phys. Rept. **492**, 1 (2010).
 - [13] S.N. Shevchenko, S. Ashhab, and F. Nori, Phys. Rev. B **85** 094502 (2012).
 - [14] L-K Kim, J-N Fuchas and G. Montambaux, arXiv:1201.1479 (unpublished); R. de Gail *et al.* arXiv:1203.1262 (unpublished).
 - [15] A. Das Phys. Rev. B **82**, 172402 (2010); S. Bhattacharya, A. Das, and S. Dasgupta, arXiv:1112.6171 (unpublished).
 - [16] A. Robertson, V.M. Galitski, and G. Refael, Phys. Rev. Lett. **106**, 165701 (2011).
 - [17] S. Pielawa, Phys. Rev. A **83**, 013628 (2011).
 - [18] D. Rokhsar and B. G. Kotliar, Phys. Rev. B **44**, 10328 (1991).
 - [19] We note that within the single site homogeneous mean-field theory, the system does not exhibit freezing for $\eta = 0$. This behavior originates from the constraint of conservation of particle number at each site and is not seen in realistic systems with traps where only the total particle number is conserved.
 - [20] D. Pekker, B. Wunsch, T. Kitagawa, E. Manousakis, A. S. Sorensen, E. Demler *et al* (unpublished).
 - [21] M. R. Andrews *et al.*, Science **275**, 637 (1997); T. Schumm *et al.*, Nat. Phys. **1**, 57 (2005); G.-B. Jo *et al.*, Phys. Rev. Lett. **98**, 180401 (2007).
 - [22] F. Gerbier, Phys. Rev. Lett. **99**, 120405 (2007); D.M. Weld *et al.*, Phys. Rev. Lett. **103**, 245301 (2009).